Astron. Astrophys. 159, 309–316 (1986)

ASTRONOMY AND ASTROPHYSICS

CO $J=4-3$ observations of molecular clouds

Glenn J. White[1], **J.P. Phillips**[1], **K.J. Richardson**[1], **and R.H. Harten**[2]

[1] Astrophysics Group, Queen Mary College, University of London, Mile End Road, London E1 4NS, England
[2] Netherlands Foundation for Radio Astronomy, Oude Hoogeveensdijk 4, Dwingeloo, The Netherlands

Received October 8, accepted November 27, 1985

Summary. A survey of the CO $J=4-3$ transition has been made towards a sample of seven galactic molecular clouds. These data have been combined with spectra for the lower CO transitions to examine how they vary in line shape with different transition. Such variations are examined using LVG modelling techniques to obtain estimates of the physical state of the emitting gas. We discuss the implications and importance that observations of these submillimetre wavelength transitions have in refining knowledge of the gas in molecular clouds.

Key words: molecular clouds – interstellar molecules

1. Introduction

Studies of the rotational molecular emission lines from interstellar carbon monoxide have been an important astrophysical tool in the study of the physical structure of interstellar molecular clouds. The majority of previous studies have been of the CO $J=1-0$ and $J=2-1$ transitions and isotopes (see for example Phillips et al., 1979), a consequence of the limited availability of submillimeter wavelength telescopes and receivers. In recent years, observations of the CO $J=3-2$ transition at 0.87 mm wavelength have become quite routine (White et al., 1981; Richardson et al., 1985a), although studies of the higher rotation transitions are much more limited, due in part to the observational problems of the high atmospheric absorption encountered from even the driest of ground-based astronomical sites.

Astrophysically, the higher rotational molecular transitions offer the chance to observe selectively higher density material. In this paper we report observations of 7 molecular clouds in the CO $J=4-3$ transition, for which we have also obtained matching CO $J=2-1$ and/or $J=3-2$ data.

2. The observations

The CO $J=4-3$ observations presented in this paper were obtained with the QMC Submillimeter Wave Heterodyne Spectrometer (White et al., 1986) mounted at the $F/9$ focus of the 3.8 meter United Kingdom Infrared Telescope (UKIRT) at Mauna Kea during the period August 31 – September 3 1983. During this observing session the zenith atmospheric transmission was measured to be greater than 0.4 for about half of the time. When the transmission at the CO $J=4-3$ frequency (460.04081 GHz) became worse than 0.4, observations were carried out of the matching CO $J=3-2$ or $J=2-1$ transitions, for which the atmospheric transmission is always better. In addition the CO $J=2-1$ and $J=3-2$ observations were supplemented by data obtained in August and September 1982, and during May and October 1983.

The total system noise temperatures (single sideband equivalent) including all optics, telescope and atmospheric losses, were typically 180 K, 350 K, and 850 K (equivalent to that for a perfect antenna above the earth's atmosphere), at the CO $J=2-1$, $3-2$, and $4-3$ frequencies, for which the beamsizes were measured to be 83″, 55″, and 42″ respectively. The velocity resolution was selectable using various filters in the IF, and is indicated in the individual channel spacings on the spectra. Observations of the moon and planets were made in order to calibrate the data, and all observations have been expressed in units of T_r^*. This scale was derived using the standard chopper wheel calibration procedure (Kutner and Ulich, 1981), and assuming the respective forward scattering efficiences $\eta_{\rm fss}$, to be 0.80, 0.88, and 0.85 for the three frequencies, determined from observations of the moon. The absolute calibrations at 230 and 345 GHz are estimated to be good to $\pm 15\%$, and $\pm 20\%$ at 460 GHz.

3. The results

The coordinates of the molecular clouds which were observed are listed in Table 1. Observations of individual regions will be discussed in the following sections.

Table 1. Coordinates of the molecular clouds observed

Source	RA (1950)	DEC (1950)
ϱ Oph A	16 23 25	−24 15 49
M 17	18 17 26	−16 14 54
S 68	18 27 57	+01 14 39
G 35.2–0.74	18 55 41	+01 36 32
W 51	19 21 27	+14 25 30
S 106	20 25 32	+37 12 25
DR 21	20 37 10	+42 09 00

Send offprint requests to: G.J. White

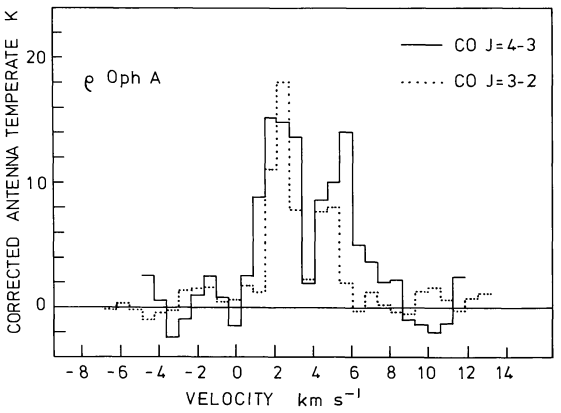

Fig. 1. CO $J=3-2$ and $4-3$ spectra of ϱ Oph A

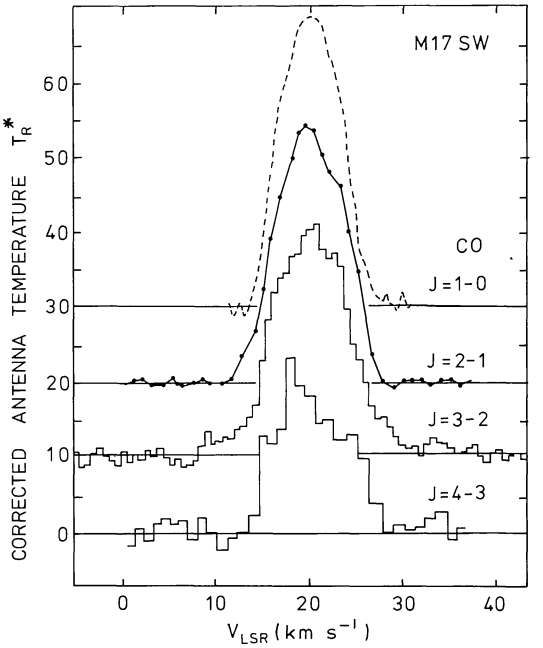

Fig. 2. CO $J=1-0$, $2-1$, $3-2$, and $4-3$ spectra of M17SW. The CO $J=1-0$ spectrum has been adapted from Kwan (1978)

3.1. ϱ Oph A

The CO distribution in the ϱ Ophiuchus cloud extends over an area of at least a quarter of a square degree, and is dominated by a number of intense CO hot spots (Loren et al., 1980). CO spectra in the $J=1-0$ and $J=2-1$ transitions have been obtained by Loren et al. (1981). These show the lines to have deep self-reversals at velocities close to 4.0 km s^{-1}, the two temperature peaks in the lines occurring at velocities of 2.2 and 5.0 km s^{-1}, with emission extending over the velocity range 0–9 km s^{-1}. Measurements of the ^{13}CO lines in this direction indicate that the optical depths in CO (and also ^{13}CO) may be very large (Lada and Wilking, 1980). In Fig. 1, spectra are shown of the CO $J=3-2$ and CO $J=4-3$ lines towards the central position in ϱ Oph A.

The peak line intensities in these higher transitions are substantially lower than the CO $J=1-0$ and CO $J=2-1$ lines, with the peak T_r^* (CO $J=3-2$) = 18.1 K and T_r^* (CO $J=4-3$) = 15.0 K. The CO $J=4-3$ line shows a weak red wing extending from 6–8 km s^{-1}, which is not detected in the spectra for the lower transitions. In the deep self-absorption dip at 3.8 km s^{-1} the minimum value of corrected antenna temperature, $T_{\rm dip}^* = 2$ K in the CO $J=4-3$ transition, is similar to that seen in the CO $J=3-2$ spectrum. In order to examine the spatial distribution of the gas in this part of the cloud we obtained a 19 point map around ϱ Oph A in the CO $J=3-2$ line. To the SE of ϱ Oph A, the emission at +5 km s^{-1} disappears at separations greater than 2 arcmin from ϱ Oph A, leaving a single dominant emission component at 3 km s^{-1}; whereas to the NW, the strength of the 5 km s^{-1} component increases sharply, whilst the 3 km s^{-1} component remains relatively constant. The kinematic structure of this region is quite complex and will be discussed in a separate and more detailed study (in preparation).

3.2. M17SW

The CO $J=1-0$, $2-1$, and $3-2$ spectra towards the M17SW molecular cloud have been discussed in some detail by Kwan (1978), Martin, Sanders and Hills (1984) and Richardson et al. (1985). In Fig. 2 we show a composite set of CO spectra including the new CO $J=4-3$ data. We are unable to confirm the high ($T_r^* = 50$ K) intensities reported by Kwan (1978) for either the CO $J=2-1$ or CO $J=3-2$ data, our own values indicating $T_r^* = 36$ K (CO $J=2-1$) and 33 K (CO $J=3-2$). These latter values are consistent with CO $J=2-1$ measurements obtained at the Kitt Peak 12 m Telescope (White and Avery, unpublished data), and with the CO $J=3-2$ data reported by Martin et al. (1984). The line intensities observed in the high J-transitions are always less than that observed in the CO $J=1-0$ transition, the CO $J=4-3$ intensity being the weakest of all. We are unable to confirm the $T_r^* = 50$ K line strength reported by Schulz et al. (1985) for the CO $J=4-3$ line at the same position, measured with a 56 arcsec beam. The line wings seen at the edge of the line core (velocity ranges 9–12 and 28–31 km s^{-1}) which are quite prominent in the CO $J=3-2$ data, are not visible in the CO $J=4-3$ data. Since we were unable to measure accurately a point-like source calibrator at the CO $J=4-3$ frequency, the coupling efficiency for small diameter objects (such as the area of high velocity emission) is not well determined, and it is consequently impossible to say whether the differences in the line profiles are a beam dependent effect, a consequence of the s/n ratio or some more intrinsic characteristic of the emission in the different transitions.

3.3. S68

In order to obtain CO $J=4-3$ data towards a region which is not known to exhibit complex spatial structure, self-absorbed or complex line profiles, we have observed the region in S68 studied by Bally and Langer (1982), designated by them as the (8,2) position. From CO $J=1-0$ data, the kinetic temperature of the gas was estimated to be >27 K. We have measured the peak T_r^* to be 15 K, 13 K and 9.5 K for the CO $J=2-1$, $3-2$, and $4-3$ transitions respectively, as shown in Fig. 3.

3.4. G35.2–0.74

This is an active star formation centre which has been discussed in some detail by Little et al. (1983, 1985), Dent et al. (1984), and White et al. (in preparation). It is known to be the site of a bipolar molecular flow, and has associated radio continuum and infrared emission. The CO $J=3-2$ and $4-3$ profiles are shown in Fig. 4

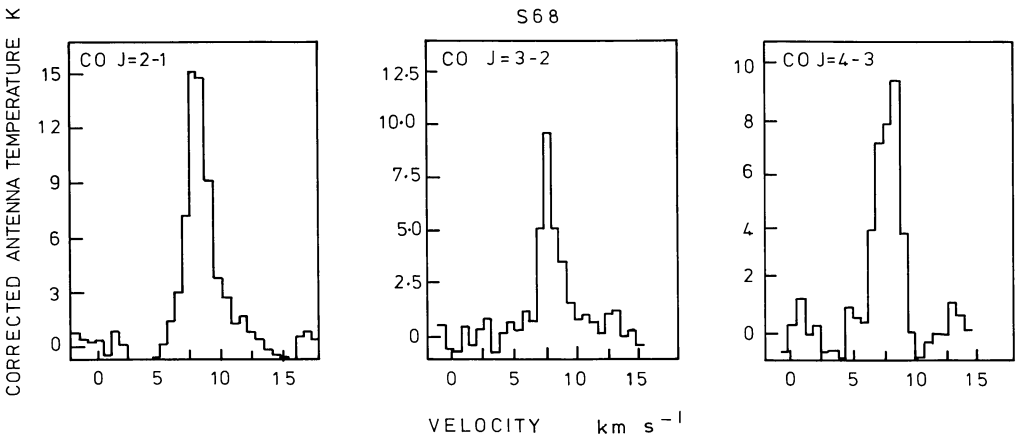

Fig. 3. CO $J=3-2$ and $3-2$, and $4-3$ spectra of S68

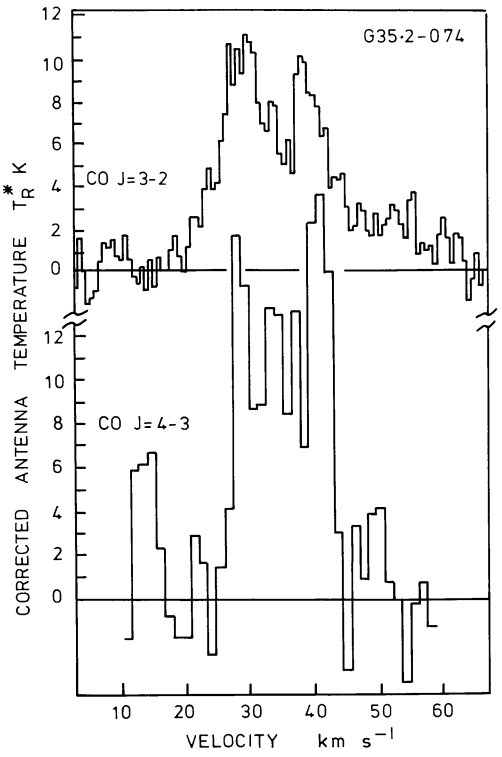

Fig. 4. CO $J=3-2$ and $4-3$ spectra of G35.2 – 0.74

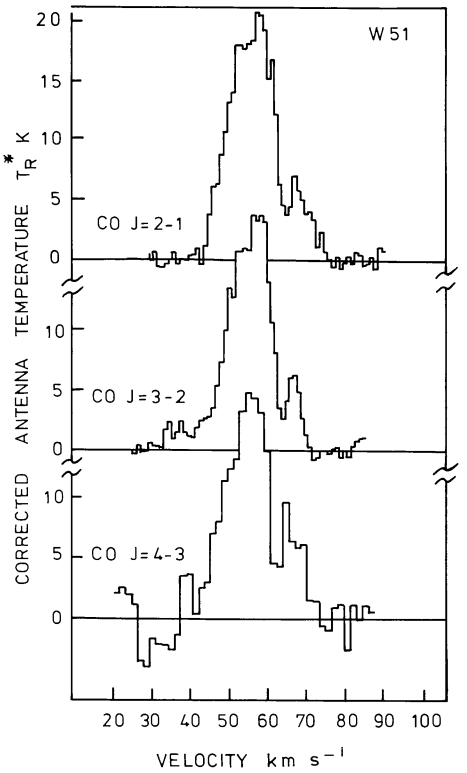

Fig. 5. CO $J=2-1$, $3-2$, and $4-3$ spectra of W51

(CO $J=2-1$ profiles have already been published by Little et al., 1983). A strong red wing is present in the CO $J=3-2$ spectrum extending from $+40$ to $+60\,\mathrm{km\,s^{-1}}$. This spectrum has a similar shape to the CO $J=2-1$ spectrum presented in Little et al. (1983), where both the self-absorption and redshifted high velocity line wings are prominent. The CO $J=4-3$ spectrum shows prominent self-absorption, with the two dominant velocity peaks lying at similar velocities to those seen at lower frequencies. However, the emission in the redshifted line wing is not clearly seen in the higher CO transition.

3.5. *W51*

This is a giant molecular complex containing several active star formation centres embedded in the core of the cloud. In Fig. 5 we show spectra of the CO $J=2-1$, $3-2$, and $4-3$ transitions. These are characterised by a broad, complex line profile, which has prominent reversal at $+62\,\mathrm{km\,s^{-1}}$. The appearance of the line is very similar in all three transitions, suggesting that the line may be optically thick over most of the spectral profile. The peak values of T_r^* are 21 K, 20 K and 19 K for the CO $J=2-1$, $3-2$, and $4-3$ transitions respectively. The depth of the self-absorption remains similar $T_{\mathrm{dip}}^* \sim 4$ K in all of the spectra. This source is the only object observed in the present survey for which the spectral profiles are broadly similar in all transitions.

3.6. *S106*

This molecular cloud is associated with a prominent bipolar nebula. The structure of the molecular cloud core is clearly seen in

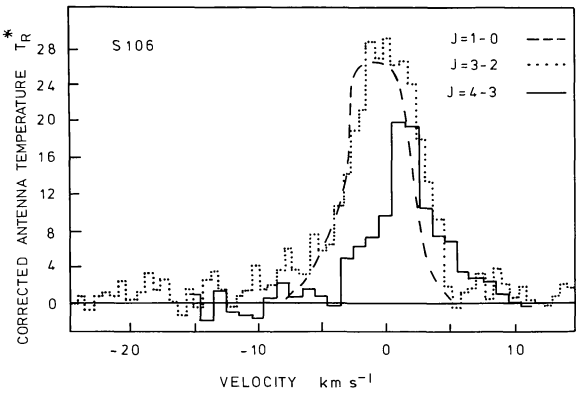

Fig. 6. CO $J=1-0$, $3-2$, and $4-3$ spectra of S106. The $J=1-0$ spectrum has been adapted from Bally and Scoville (1982)

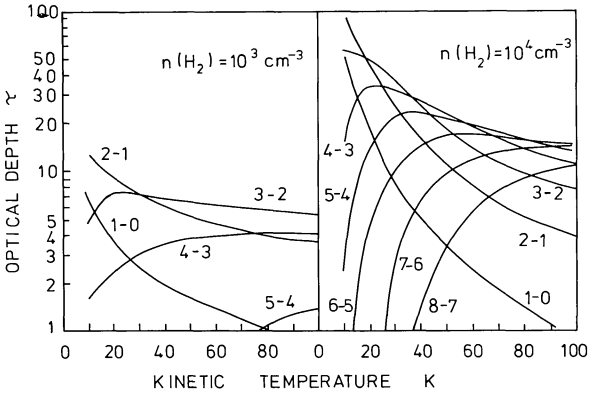

Fig. 8. LVG calculations of optical depth as a function of temperature. The calculations for different transitions are indicated as solid lines on the plot, for two values of hydrogen density

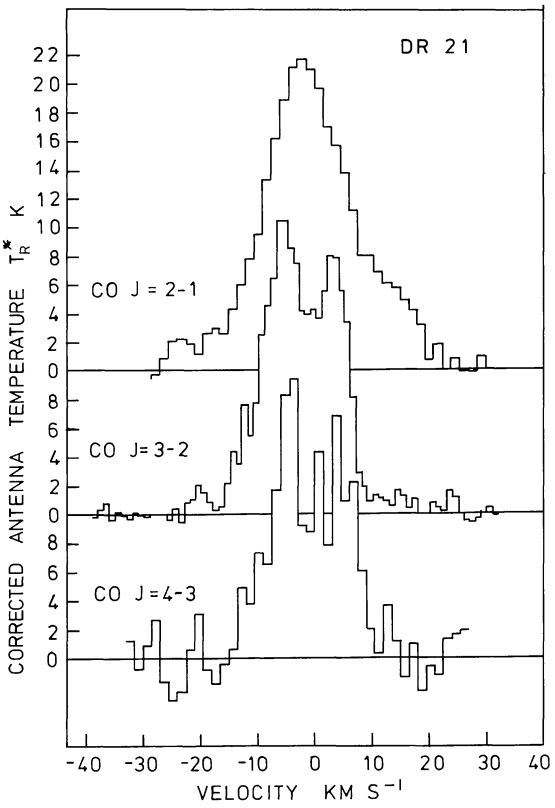

Fig. 7. CO $J=2-1$, $3-2$, and $4-3$ spectra of DR21

the data of Little et al. (1983). In Fig. 6 we show spectra in the CO $J=1-0$ transition (adapted from Bally and Scoville, 1982), and our own CO $J=3-2$ and $4-3$ data. The $J=3-2$ data show a strong blue shifted wing [this can also be seen in the unpublished CO $J=2-1$ data of Little et al. (private communication)]. The central lsr velocity of the line core becomes progressively higher with increase in the J-transition. The CO $J=1-0$ and $3-2$ transitions have similar values of T_r^* of ~ 25–28 K, whereas the CO $J=4-3$ value is about 20% less. The blue shifted side of the CO $J=4-3$ line is substantially lower in intensity than for the lower transitions.

3.7. DR21

This is a complex region consisting of several molecular cores embedded in a giant molecular cloud. A more complete mapping of this area in the CO $J=2-1$ and $3-2$ transition has been presented in a separate paper (Richardson et al., 1986, and other observations reported by Plambeck et al. (1983). CO $J=2-1$, $3-2$, and $4-3$ profiles observed at the centre of the density maximum in DR21 are shown in Fig. 7.

These data show that self reversal dips are present in the CO $J=3-2$ and $4-3$ spectra, but not in the $J=2-1$ transition. A similar effect was also reported by Phillips et al. (1981) at a nearby position in DR21, who also found that no self-absorption was seen in matching CO $J=1-0$ spectra. The basic line shapes of the CO $J=2-1$, $3-2$, and $4-3$ transitions in the central regions of the line core (excluding the velocity ranges corresponding to the self-reversal) remain similar from transition to transition, the emission in the line wings (in the velocity ranges -25 to $-15\,\mathrm{km\,s^{-1}}$ and $+10$ to $+20\,\mathrm{km\,s^{-1}}$) being much weaker in the higher J-transitions than in the CO $J=1-0$ and $2-1$ data.

4. Discussion

Comparison of spectral profiles and intensities in the different rotational transitions of a molecular species offers a potentially powerful means of determining the excitation, and physical conditions in the cores of molecular clouds. We will discuss the observations reported here in terms of simple models of molecular line formation.

For a molecular species such as carbon monoxide, which is found to be optically thick towards most clouds, the emitted line profiles are both complex and difficult to model uniquely. This is because for a given spectral profile, the emitted lineshape is particularly dependent on the velocity field within the cloud, and also on the variation of excitation temperature and opacity. In addition, the opacity itself may be a strong function of density, kinetic temperature and rotational transition. This can be seen in Fig. 8, where we have carried out a large velocity gradient (LVG) analysis for the CO molecule (Goldreich and Kwan, 1974) to determine the variation of optical depth with temperature for J-transitions up to the $J=8-7$. This model assumes a plausible value of the molecular abundance per unit velocity gradient, $X/dV/dR = 5\ 10^{-5}\,\mathrm{pc\,km^{-1}\,s}$. It is seen that for the CO $J=4-3$ transition, the opacity becomes less than unity for kinetic

temperatures <10 K, and densities $<10^3$ cm^{-3}. This arises due to lack of sufficient excitation of the CO molecule for population of the $J=4$ level. Such conditions may prevail, in particular, within the outer regions of molecular clouds. The critical densities for thermalisation of CO in the CO $J=1-0$, $2-1$, $3-2$, and $4-3$ transitions are $2\ 10^3$, 10^4, $4\ 10^4$, and $1.5\ 10^5$ cm^{-3} respectively (Evans, 1979). As a result the effects of CO $J=4-3$ self-absorption due to the cool, less dense foreground material might be expected to be small, or considerably reduced. However, even at densities as low as 10^3 cm^{-3}, τ(CO $J=4-3$) can still be greater than unity for kinetic temperatures in the range 10–100 K, and consequently we would still expect to see evidence of self-absorption. Of the sources observed in this survey, the spectra suggest that we may be seeing self-absorption effects in the profiles of ϱ Oph A, G35.2–0.74, DR 21, W49 and DR 21 (OH). It is likely that the effects of self-absorption may also modify the profile shape of M17.

A general characteristic of many of the CO $J=4-3$ profiles is for them to be less intense than many of their respective matching lower transition data. This is particularly noticeable for S106 and M17. Such a trend may be a consequence of the differing beam sizes used in the comparison, or alternatively of sub-thermal or non-LTE excitation of the CO. In the cases of M17 and S106, the decrease in line strength is seen to occur over much of the core of the line profile, and does not appear to be related to a clearly recognisable self-absorption dip. Examples of sources in this survey for which such dips can clearly be seen include ϱ Oph A, G35.2–0.74, W51 and DR 21.

To examine the overall characteristics and trends indicated by our data, we have carried out LVG modelling for a number of the objects observed. Although such an approximation is undoubtedly an oversimplification for real molecular cloud cores it is still probably reasonable in approximating the local excitation conditions, and provides a computationally simple way of solving the radiative transfer. More detailed comparison of the various techniques has been given by White (1977) and Richardson (1985). We will now examine several sources in more detail.

4.1. S68

This CO hot spot was mapped in the survey of Loren et al. (1979), and subsequently by Bally and Langer (1982). We have applied LVG calculations both to this data, and the present CO $J=4-3$ observations. Models with kinetic temperatures >25 K give poor agreement between the CO $J=1-0$ data and the CO $J=4-3$ intensity, the CO $J=1-0$ line being typically 30–50% too intense relative to the other lines. For kinetic temperatures <25 K, the calculated intensities approach agreement with the data (after allowing for absolute calibration uncertainties) for $n(H_2)<3\ 10^3$ cm^{-3} and $X/(dV/dR)>10^{-5}$ km^{-1} s pc. Since the contour values of equal predicted antenna temperatures for the different transitions, when plotted on a grid of $X/(dV/dR)$ against $n(H_2)$, run virtually parallel to each other, we can use the CO $J=1-0$ isotope ratios estimated by Bally and Langer (1982) to confine the possible range of solutions to $800<n(H_2)<4000$ cm^{-3}, and $1\ 10^{-4}>X(CO)>5\ 10^{-4}$ (where we assume the velocity gradient, (dV/dR), is given from the linewidth and the observed cloud size, for all values of isotope ratios $89<[CO]/[^{13}CO]<40$ and $1000<[CO]/[C^{18}O]<500$. Under these conditions both CO and ^{13}CO have optical depths greater than 1, although T_{ex} is less than the kinetic temperature. For this situation, and using the CO $J=1-0$ antenna temperatures reported by Bally and Langer (1982), we then find $\tau(^{13}CO)=0.25$, and τ(CO) is therefore $\gg 1$.

4.2. S106

S106 has been mapped in considerable detail by Bally and Scoville (1982) in the CO $J=1-0$ line, and by ourselves (Kaifu et al., in preparation) in the CO $J=3-2$ transition. At positions close to the cloud core, marked variations are seen in the shape of the spectral profiles, particularly in the mid-velocity CO lying within ~ 5 km s^{-1} from the line centre. This suggests the presence of small scale structure at the limit of resolution with the present telescope beam sizes. The CO $J=4-3$ spectrum has a strikingly different line shape to that of the lower transitions, with a marked reduction in the line strength, and a redshifting of the line centre velocity. From CO $J=1-0$ data we will assume the kinetic temperature is 36 K in the centre of the molecular cloud. Under these conditions, the predicted CO abundance and densities in the emitting gas are respectively $2\ 10^{-5}$ km^{-1} s pc, and $n(H_2)=10^4$ cm^{-3}. For velocities <0 km s^{-1}, the emission originates from a region with lower density, and either a higher value of X(CO), or a decreasing excitation temperature for the higher velocity gas. Support for the lower excitation temperature and reduced filling factor explanation may be found from observational studies towards several other high velocity sources (Snell et al., 1984). Such a situation is not however always the case, and for several of the sources, CO $J=3-2$ measurements may imply a higher excitation temperature in the high velocity gas than in the surrounding ambient material (Phillips et al., 1982; White et al., 1981). It is unlikely that S 106 is an example of this latter category.

4.3. W51

The CO spectra towards W51 are seen to contain evidence for a deep self-reversal dip at a velocity of 62 km s^{-1}. For most interstellar molecular clouds, self-reversal can arise when foreground material lies in projection against a background emitting cloud core. In this case, if the self-absorbed profile arises due to the presence of cool (or more generally, lower excitation) foreground gas, the antenna temperature at the centre of the self-absorption dip (assumed to be resolved by the telescope beam), T^*_{dip}, is given to first order by the relationship

$$T^*_{dip}=T^*_{BG}\exp(-\tau_A)+T^*_A(1-\exp(-\tau_A)) \quad (1)$$

where the quantities marked with an asterisk, *, are defined by the relationship

$$T^*=\frac{h\nu}{k}\left[\left\{\exp\left(\frac{h\nu}{kT}\right)-1\right\}^{-1}-\left\{\exp\left(\frac{h\nu}{kT_{BB}}\right)-1\right\}^{-1}\right] \quad (2)$$

and T_{BB} is the microwave background temperature, T_{BG} is the brightness temperature of the background (assume optically thick emission) source and T_A is the excitation temperature of the foreground (absorbing) cloud. In the following discussion, T_{BG} will be assessed from the observations, and T_A and τ_A evaluated for a variety of gas kinetic temperatures using LVG modelling.

W51 represents a particularly interesting example of a self-absorbed source since, for this case, the central velocity of the absorption dip is displaced by approximately 8 km s^{-1} from the centre of the main emission line. By assuming the variation of T_{BG} with v_{lsr} to be symmetric about the peak of the CO line, it is possible to estimate the value of $T_{BG}\sim 20$ K at the velocity corresponding to the centre of the self-absorption dip, assuming that both the

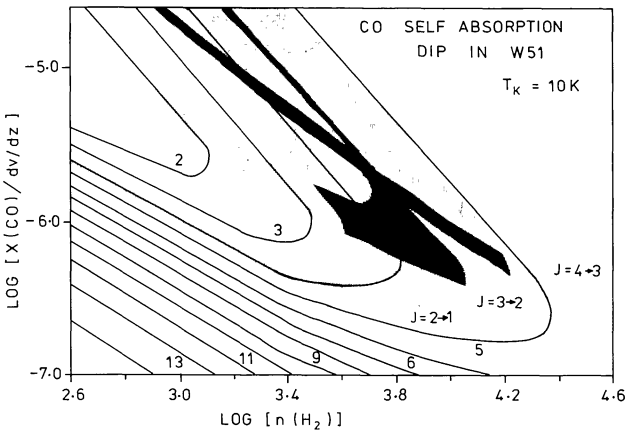

Fig. 9. LVG calculation showing (hatched areas) allowable solutions for the observed antenna temperatures in the W51 self absorption dip, for the CO $J=2-1$, $3-2$, and $4-3$ transitions

background emission and foreground absorbing material are extended with respect to our telescope beams (Phillips et al., 1981).

We can then go on to use an LVG analysis, modified as discussed above, to estimate the excitation conditions of the material giving rise to the absorption dip. The results of this analysis are illustrated in Fig. 9, where the broad areas of parameter space corresponding to specific ranges of T_r^* $(J\rightarrow J-1)$ are represented by the shaded areas, corresponding to $\pm 10\%$ error uncertainties. There are at least two notable features of this analysis. In the first place, relatively small errors in the value of $T_{\rm dip}$ for the CO $J=1-0$, $2-1$ and $3-2$ cases lead to large uncertainties in the estimates for density and $X/(dV/dR)$, and the lower frequency transitions alone would enable only an ill-defined solution to be found. By way of contrast, the area of parameter space corresponding to the observed antenna temperature in the CO $J=4-3$ line enables the area for which there are allowable solutions to be substantially reduced. When all three of the results in Fig. 9 are superimposed, the resulting permitted solutions exist over a small range of values centred on $n(H_2)\sim 5000\,{\rm cm}^{-3}$ and $X/(dV/dR)=2\ 10^{-6}\,{\rm km}^{-1}\,{\rm s\,pc}$. The case of W51 illustrates the utility of observing as wide a range of CO transitions as possible to constrain excitation conditions.

The ability to estimate the excitation temperature however is rather less precise, and may require further observations of this source at even higher frequencies – although it is apparent that solutions in the case of the foreground absorbing material are not available for $T_{\rm kin}>15\,{\rm K}$. For this source, at least, the kinetic temperature of the foreground gas must be less than that in the emission core – although as we shall see later, this may not always be the case for all sources.

On the assumption that the emitting gas at the line peak at $58\,{\rm km\,s}^{-1}$ is unabsorbed by foreground material, and assuming $T_{\rm kin}=30\,{\rm K}$, from the observed line strengths, then LVG analysis yields values of $X({\rm CO})/(dV/dR)=1.8\ 10^{-7}\,{\rm km}^{-1}\,{\rm s\,pc}$, and $n(H_2)=7.5\ 10^4\,{\rm cm}^{-3}$. These values are not uniquely defined however, and a whole range of solutions with $X/(dV/dR)=0.01\ n(H_2)^{-2}$ is possible for kinetic temperatures $<40\,{\rm K}$. Broadly speaking, therefore, it is possible to model the lines in Fig. 5 in terms of a two-component source, with a low-temperature halo, and a higher temperature core. In reality of course, neither temperature or density are likely to be discontinuous in this way, and W51 is likely to contain appreciable gradients in both these parameters. The more complex radiative transfer modelling required to incorporate such complexity is however inappropriate to this limited set of data.

Finally, it is interesting to note that if the commonly assumed molecular abundance ratio, $X({\rm CO})=5\ 10^{-5}$ is adopted, and the cloud velocity gradient is taken to be

$$\frac{dV}{dR}=\left(\frac{8}{3}\pi M_{H_2}\langle n(H_2)\rangle G\right)^{0.5}, \tag{3}$$

where $\langle n(H_2)\rangle$ is the mean gas density within radius R, M_{H_2} is the cloud mass and G the gravitational constant, we then determine

$$X({\rm CO})/(dV/dR)=1.7\ 10^{-3}/(\langle n(H_2)\rangle)^{0.5}\,{\rm km}^{-1}\,{\rm s\,pc}. \tag{4}$$

An interesting feature of expression (3) is that it applies, to within small factors, for a large range of physical circumstances, whether the cloud is in free-fall collapse, supported by rotation, or in turbulent pressure equilibrium. Nevertheless, expression (4) is not consistent with any of the solutions for $X/(dV/dR)$ and $n(H_2)$ relevant to W51 (or DR21 as we shall see later). It is therefore apparent that we may be dealing with absorbing zones which are either strongly disturbed (by for example stellar winds), or which have small values for $X({\rm CO})$, an order of magnitude less than normally assumed for interstellar clouds (Richardson et al., 1985a).

4.4. DR21

Towards this source the self-absorption appears to be centrally located within the DR21 line profile, occurring at a velocity of $-1\,{\rm km\,s}^{-1}$, and having an absorption linewidth of $5\,{\rm km\,s}^{-1}$ $T_{\rm dip}$ at this velocity becomes lower with increasing J-transition, having values of 22, 14, and 9 K for the CO $J=2-1$, $3-2$, and $4-3$ transitions respectively. However, at a velocity of $-6\,{\rm km\,s}^{-1}$, just away from the absorption feature, the CO line intensity is relatively invariant with J-transition. The profile shapes for the lowest three CO transitions were discussed in detailed by Richardson et al. 1986, in particular the observations that the CO $J=3-2$ spectrum of this source is self-reversed, while the CO $J=2-1$ is not. As described in that work, these characteristics can be described in terms of a simple two-component model in which radiation from thermalised and optically thick background material passes through a hotter, but less dense, foreground gas. Both these components could be situated in the cloud core and correspond, for example, to a two-phase clump/interclump medium. The less dense gas would absorb in the CO $J=3-2$ and higher transitions, but would emit in the CO $J=1-0$ and $2-1$ lines. The full details of the model will not be repeated here, and the reader is referred to Richardson et al. (1986). We simply note that the CO $J=4-3$ data are in good agreement with the predictions of that model. An illustrative example of a fit to the observations is given in Table 2, for background material having $T_{\rm kin}=28\,{\rm K}$, foreground material with $T_{\rm kin}=38\,{\rm K}$, density $n(H_2)=2500\,{\rm cm}^{-3}$ and $X({\rm CO})/(dV/dR)=10^{-5}\,{\rm km\,s\,pc}$. The agreement between observations and the model predictions are well within the margins of error due to uncertainties in the beam coupling efficiencies.

4.5. M17

The CO $J=1-0$, $2-1$, and $3-2$ lines for M17 show a broadly similar overall shape, although the CO $J=1-0$ transition is more intense than any of the higher transitions. For an assumed $T_{\rm kin}$ of 40 K (chosen to match the CO $J=1-0$ line intensity), LVG analysis of the lowest three transitions is consistent with a range of

Table 2. Comparison of DR 21 intensities with a simple two component model. Background material: $T_{BG}=28$ K (thermalised, optically thick). Foreground material: $T_A=38$ K, $X_{CO}/(dv/dr)=10^{-5}$, $n_{H_2}=2.5\ 10^3\,cm^{-3}$

CO transition	T^*_{BG}		T^*_{DIP}	
	Predicted	Observed[a]	Predicted	Observed[b]
$J=1-0$	24.5	20.0[c]	26.4	25.0[c]
$J=2-1$	22.7	19.0	22.2	21.5
$J=3-2$	20.5	20.5	17.2	14.0
$J=4-3$	18.4	19.0	10.6	9.0

[a] At $V_{LSR}=-6\,kms^{-1}$
[b] At $V_{LSR}=-1\,kms^{-1}$
[c] Plambeck et al. (1983)

solutions having $X/(dV/dR)>30\,n(H_2)^{-1.5}$. However, this relationship gives poor agreement with the predicted CO $J=4-3$ line strength, which is about twice as strong as the observations indicate. It is therefore unlikely that LVG analysis of this source is useful, particularly in view of the discussion given by Martin et al. (1984).

The data in Fig. 2 show a trend in the linewidth, the FWHM increasing with J-transition, with $\Delta v(CO\,J=2-1)=1.16\Delta v$ (CO $J=1-0$), $\Delta v(CO\,J=3-2)=1.24\,\Delta v$ (CO $J=1-0$) and $\Delta v(CO\,J=4-3)=1.32\Delta v(CO\,J=1-0)$. This broadening is consistent with that expected for a medium subject to gradients in velocity and density, in which the opacity varies with transition; a high CO $J=2-1$ opacity for instance would ensure that we sample a larger volume of material and a larger range of velocities, than for lower opacity transitions.

The changes in line profile may however also be suggestive of a second hypothesis outlined by Phillips et al. (1979). In this case the variation of line width with transition is a consequence of microturbulent broadening, the varying linewidths reflecting increasing levels of saturatiion. Under these circumstances, and given that $\tau(CO\,J=1-0)$ is almost certainly $\gg 1$, then the linewidth $\Delta v(J\to J-1)\propto(\ln\tau(J\to J-1))^{0.5}$. To test whether this is relevant to the present circumstances, we shall adopt a velocity gradient $(dV/dR)=2\,kms^{-1}\,pc^{-1}$ (from the observed source size reported by Thronson and Lada (1983) and the linewidth), and take as an example an abundance $X(CO)\sim 10^{-4}$. We then determine $n(H_2)\sim 70000\,cm^{-3}$. Taking this lower limit value to represent the true density, we then estimate $\Delta v(J=2-1/1-0)=1.20$, $\Delta v(J=3-2/1-0)=1.26$ and $\Delta v(J=4-3/1-0)=1.26$, in reasonable accord with the observations. Thus, allowing for uncertainties in the observations and precise details of the technique, we are nonetheless able to reproduce the observed trends.

We note at this point that whilst we have employed LVG modeling for most of the analysis, the results should be broadly similar to those derived from corresponding turbulent models, for which the analysis of Phillips et al. (1979) was also developed. For that case we would require the velocity gradient $=\Delta v_{turb}/2R$, where R is the cloud diameter and Δv_{turb} is the relevant range of turbulent velocities.

To summarise, we find that the observed trends in linewidth and profile shape are probably best represented by a model in which the density and excitation decreases from the source core, and in which the lines broaden through a process of saturation. In almost all relevant models we find that the opacity increases rapidly between the CO $J=1-0$ and CO $J=2-1$ transitions, and then more slowly up to the CO $J=3-2$ and $J=4-3$ transitions. This is reflected in a similar trend in the observed linewidths.

5. Conclusions

1. CO $J=4-3$ data have been observed towards a sample of molecular clouds. The CO $J=4-3$ lines are in general less intense than their lower transition counterparts, and are often more subject to the effects of self-reversal or saturated line broadening.

2. In the self-absorbing gas associated with ϱ Oph A, W51, W49 and G35.2–0.74, the observations are consistent with the presence of cool, dense foreground absorbing material. In contrast, the data for DR 21 suggest that hotter foreground gas (or perhaps a warm interclump medium in the core of the molecular cloud) exists, which acts to remove any self-absorption in the CO $J=2-1$ transition, whilst allowing the presence of such a feature in the CO $J=3-2$ and $4-3$ transitions.

3. The linewidths observed towards M17 are found to be consistent with models in which the observed line shape results either from cicroturbulent broadening, or alternatively in an area with strong density and/or excitation gradients.

Acknowledgements. We thank the staff of UKIRT for excellent support at the telescope; PATT for the award of telescope time, and for travel and subsistence awards; the SERC for support of submillimetre astronomy and receiver development at QMC, and for fellowships for JPP and KJR; and to Dr. Lorne Avery for assistance with the observations, and for commenting on the manuscript.

References

Bally, J., Langer, W.D.: 1982, *Astrophys. J.* **255**, 143
Bally, J., Scoville, N.Z.: 1982, *Astrophys. J.* **255**, 497
Dent, W.R.F., Little, L.T., White, G.J.: 1984, *Monthly Notices Roy. Astron. Soc.* **210**, 173
Dent, W.R.F., Little, L.T., Kaifu, N., Ohishi, M., Suzuki, S.: 1985, *Astron. Astrophys.* (in press)
Evans, N.J.: 1979, in *Interstellar Molecules Proc. IAU Symp.* **87**, ed. B.H. Andrew
Goldreich, P., Kwan, J.: 1974, *Astrophys. J.* **189**, 441
Kutner, M.L., Ulich, B.L.: 1981, *Astrophys. J.* **250**, 341
Kwan, J.: 1978, *Astrophys. J.* **223**, 147
Lada, C.J., Wilking, B.A.: 1980, *Astrophys. J.* **238**, 620
Little, L.T., Brown, A.T., Riley, P.W., Matthews, N., Macdonald, G.H., Vizard, D.R., Cohen, R.J.: 1983, *Monthly Notices Roy. Astron. Soc.* **203**, 409
Little, L.T., Dent, W.R.F., Davies, S.R., White, G.J.: 1985, *Monthly Notices Roy. Astron. Soc.* **217**, 227
Loren, R.B., Wootten, A., Sandquist, A., Bernes, C.: 1980, *Astrophys. J.* **240**, L165
Loren, R.B., Plambeck, R.L., Davies, J.H., Snell, R.L.: 1981, *Astrophys. J.* **245**, 495
Martin, H.M., Sanders, D.B., Hills, R.E.: 1984, *Monthly Notices Roy. Astron. Soc.* **208**, 35
Phillips, J.P., White, G.J., Ade, P.A.R.A., Cunningham, C.T., Richardson, K.J., Robson, E.I., Watt, G.D.: 1982, *Astron. Astrophys.* **116**, 130

Phillips, T.G., Huggins, P.J., Wannier, P.G., Scoville, N.Z.: 1979, *Astrophys. J.* **231**, 720
Phillips, T.G., Knapp, G.R., Huggins, P.J., Werner, M.W., Wannier, P.G., Neugebauer, G., Ennis, D.: 1981, *Astrophys. J.* **245**, 512
Richardson, K.J., White, G.J., Avery, L.W., Lesurf, J.C.G., Harten, R.H.: 1985a, *Astrophys. J.* **290**, 637
Richardson, K.J., White, G.J., Phillips, J.P., Avery, L.W.: 1986, *Monthly Notices Roy. Astron. Soc.* **219**, 167
Richardson, K.J.: 1985, Ph.D. Thesis, University of London
Schulz, A., Gillespie, A.R., Krugel, E.: 1985, *Astron. Astrophys.* **142**, 363
Snell, R.L., Scoville, N.Z., Sanders, D.B., Erickson, N.R.: 1984, *Astrophys. J.* **284**, 176
Thronson, H.A., Lada, C.J.: 1983, *Astrophys. J.* **269**, 175
White, G.J., Phillips, J.P., Watt, G.D.: 1981, *Monthly Notices Roy. Astron. Soc.* **197**, 745
White, G.J., Monteiro, T.S., Richardson, K.J., Griffin, M.J., Rainey, R.: 1986, *Astron. Astrophys.* (in press)
White, R.E.: 1977, *Astrophys. J.* **211**, 744